

LETTER • OPEN ACCESS

Impacts of the 2017 flash drought in the US Northern plains informed by satellite-based evapotranspiration and solar-induced fluorescence

To cite this article: Mingzhu He *et al* 2019 *Environ. Res. Lett.* **14** 074019

View the [article online](#) for updates and enhancements.

Environmental Research Letters

**LETTER****OPEN ACCESS****RECEIVED**
5 February 2019**REVISED**
10 May 2019**ACCEPTED FOR PUBLICATION**
20 May 2019**PUBLISHED**
12 July 2019

Original content from this work may be used under the terms of the [Creative Commons Attribution 3.0 licence](#).

Any further distribution of this work must maintain attribution to the author(s) and the title of the work, journal citation and DOI.



Impacts of the 2017 flash drought in the US Northern plains informed by satellite-based evapotranspiration and solar-induced fluorescence

Mingzhu He^{1,8}, John S Kimball^{1,2}, Yonghong Yi³, Steve Running¹, Kaiyu Guan⁴, Kelsey Jensco⁵, Bruce Maxwell⁶ and Marco Maneta⁷

¹ Numerical Terradynamic Simulation Group, W.A. Franke College of Forestry & Conservation, University of Montana, Missoula, MT 59812, United States of America

² Department of Ecosystem and Conservation Sciences, W.A. Franke College of Forestry & Conservation, University of Montana, Missoula, MT 59812, United States of America

³ Jet Propulsion Laboratory, California Institute of Technology, 4800 Oak Grove Drive, Pasadena, CA 91109, United States of America

⁴ Department of Natural Resources and Environmental Sciences, University of Illinois at Urbana-Champaign, Urbana, IL 61820, United States of America

⁵ Department of Forest Management, College of Forestry & Conservation, University of Montana, Missoula, MT 59812, United States of America

⁶ Department of Land Resources and Environmental Science, Montana State University, Bozeman, MT 59717, United States of America

⁷ Department of Geosciences, University of Montana, Missoula, MT 59812, United States of America

⁸ Author to whom any correspondence should be addressed.

E-mail: mingzhu.he@ntsg.umt.edu

Keywords: drought, cropland, evapotranspiration, solar-induced fluorescence, crop production

Abstract

Drought is increasing in frequency and severity, exacerbating food and water security risks in an era of continued global warming and human population growth. Here, we analyzed a severe summer drought affecting the US Northern Plains region in 2017. We examined the spatial pattern and seasonal progression of vegetation productivity and water use in the region using satellite-based estimates of field-scale (30 m) cropland evapotranspiration (ET), county level annual crop production statistics, and GOME-2 satellite observations of solar-induced chlorophyll fluorescence (SIF). The cropland ET record shows strong potential to track seasonal cropland water demands spatially, with strong correspondence to regional climate variables in the Northern Plains. The GOME-2 SIF record shows significant but limited correlations with finer scale climate variability due to the coarse sensor footprint, but captured an anomalous regional productivity decline coincident with drought related decreases in crop production and ET. The drought contributed to an overall 25% reduction in cropland ET, 6% decrease in crop production, and 11% reduction in SIF productivity over the region from April to September in 2017 relative to the longer (2008–2017) satellite record. More severely impacted agricultural areas indicated by the US Drought Monitor exceptional drought (D4) category represented 11% of the region and showed much larger anomalous ET (20%–81%) and productivity (11%–73%) declines. The regional pattern of drought impacts indicated more severe productivity and ET reductions in the north central and southern counties with extensive agriculture, and less impact in the western counties of the Northern Plains. This study provides a multiscale assessment of drought related impacts on regional productivity and ET over a crop intensive region, emphasizing the use of global satellite observations capable of informing regional to global scale water and food security assessments.

1. Introduction

Global warming is enhancing the frequency and severity extreme climatic events including drought

(Hao *et al* 2013, AghaKouchak *et al* 2014, Trugman *et al* 2018), which is one of the most complex and costliest natural disasters affecting humans and the environment (Luo and Wood 2007, Mishra and

Singh 2010, Wang *et al* 2014). Large-scale droughts have been reported to weaken the terrestrial carbon sink and intensify competition between food demand and biofuel production (Zhao and Running 2010). Drought often shows direct and immediate impacts on agricultural land due to the strong dependence of various stages of crop growth on water resources (Narasimhan and Srinivasan 2005, Martínez-Fernández *et al* 2016, Peng *et al* 2018), severely influencing crop production and food security (Lobell *et al* 2011, Trnka *et al* 2012, Madagdar *et al* 2017). For example, the negative effects of drought resulted in 0.1%–1.2% reductions in annual corn and soybean yields in dryland counties in the United States from 2001 to 2013, while irrigated counties showed slightly smaller (0.1%–0.5%) reductions in annual crop yields (Kuwayama *et al* 2018). Less frequent, but more extreme drought events have had a much larger impact on agricultural productivity and economic losses, even in regions with a relatively well developed water management infrastructure. For example, a recent severe drought was reported to have cost the California agricultural industry \$1.5 billion in 2014 (Howitt *et al* 2014).

Flash drought usually occurs with decreased soil moisture associated with anomalously high temperatures and increases in evapotranspiration (ET) (Mo and Lettenmaier 2015, Otkin *et al* 2018). It is difficult to predict and has a substantial impact on agricultural lands due to the extreme heat or precipitation deficit associated with its occurrence (Gerken *et al* 2018, Otkin *et al* 2018). In 2017, the US Drought Monitor (USDM, Svoboda *et al* 2002) documented a particularly severe flash drought over the Northern Plains region of the continental US (CONUS), with about 83% of the total land area experiencing abnormally dry conditions, which severely impacted the agricultural industry. Agriculture is the leading industry in the Northern Plains, contributing about \$4.39B, \$7.56B, \$6.05B and \$1.72B to the economy in 2016 for the states of MT, ND, SD and WY, respectively. Thus, agriculture is a very important economic force in the Northern Plains. However, relatively few studies have explored the impact of the recent drought on croplands in the Northern Plains, while detailed climate impact assessments and capabilities for regional monitoring are constrained by a relatively sparse regional weather station network (Horel and Dong 2010). Alternatively, consistent multi-scale satellite observational records may provide a new perspective on the regional impact of the 2017 drought on croplands across the Northern Plains. These records include field scale cropland ET and regional scale solar-induced chlorophyll fluorescence (SIF) observations that are sensitive to land use and climate variability, and provide continuous observations over multiple years and the entire region. When used on context with other available information, these observations may provide

an effective assessment of drought related impacts on cropland water use and productivity.

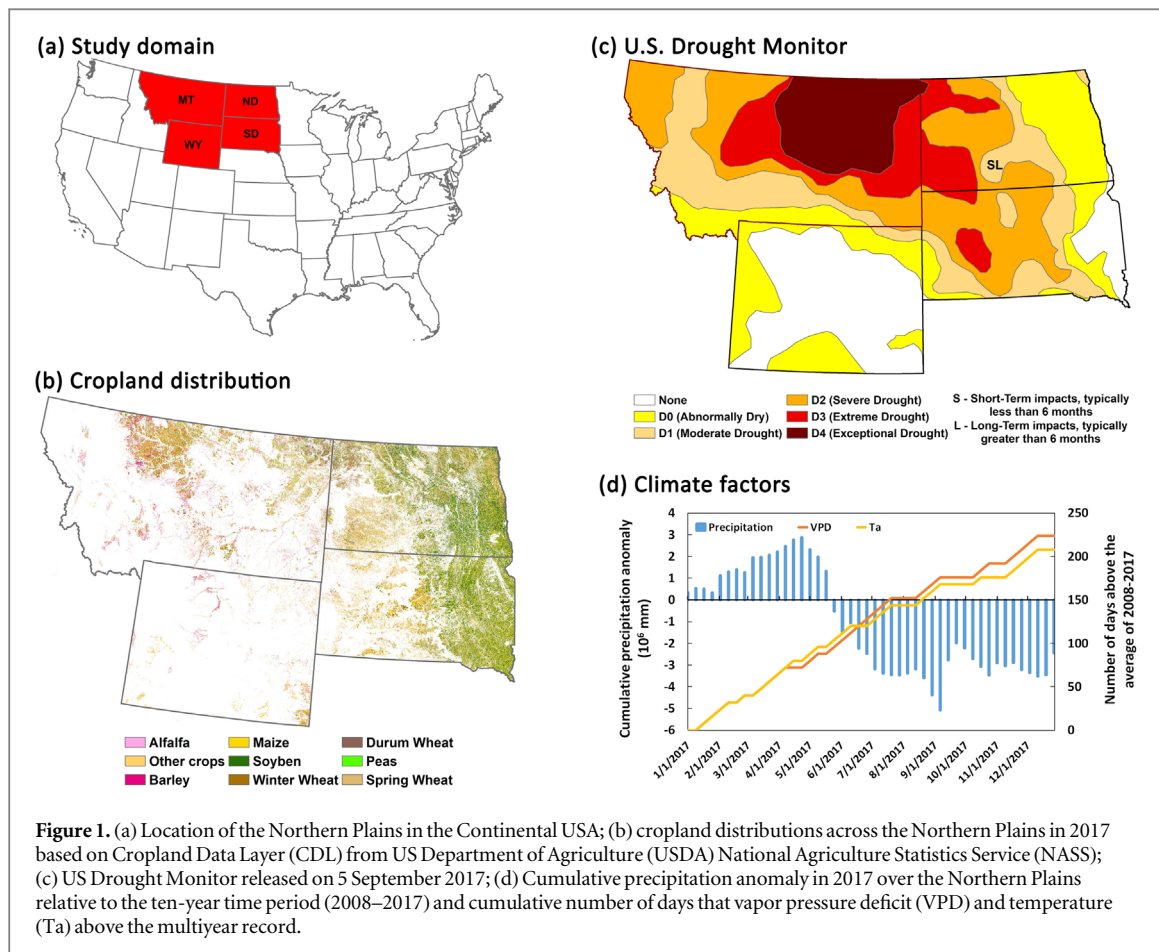
In this study, we evaluated the impact of the 2017 Northern Plains flash drought on regional cropland ET and productivity (figure 1). A satellite-based 30 m 8 d CONUS cropland ET record (He *et al* 2019) was used with coarser (0.5°) monthly SIF observations from the GOME-2 satellite (Joiner *et al* 2016) to characterize the patterns and seasonal changes in cropland water use and productivity. The satellite observations were used with reported county-level crop production and available climate data to characterize drought related impacts relative to the recent historical record (2008–2017). The following sections provide a description of the Northern Plains and summary of the data and methods used in this study (section 2), a presentation of the major results from this investigation (section 3), and a concluding discussion of the study implications for regional drought monitoring and agricultural water management (section 4).

2. Materials

2.1. Study domain and the USDM

The domain for this study includes the CONUS northern-tier states of the Northern Plains (figure 1(a)), including Montana (MT), Wyoming (WY), North Dakota (ND) and South Dakota (SD). The region encompasses the epicenter of the 2017 Northern Plains summer flash drought according to the USDM (figure 1(c)). Croplands accounted for about 28%–32% of the total land area of the Northern Plains from 2008 to 2017, with the largest area planted in 2017 (5.24×10^7 hectares) and the smallest area in 2011 (4.59×10^7 hectares). The major crops in this region include alfalfa, barley, wheat (spring, winter, durum), maize, and soybeans, which were mainly distributed in northern and eastern MT, eastern ND and SD in 2017 (figure 1(b)).

The USDM (Svoboda *et al* 2002) has been used as a benchmark for the identification of drought (Ford *et al* 2015, Schroeder *et al* 2016), providing a weekly map assessment showing the occurrence, spatial extent and relative severity of drought over the CONUS domain. The USDM is determined from expert assessments using climatological, hydrological and satellite-based information, including the Palmer Drought Severity Index, Standardized Precipitation Index, satellite-based assessments of vegetation health, and various indicators of soil moisture. According to the USDM, the study domain experienced a severe summer flash drought in 2017. The largest influencing areas of drought (D0: abnormally dry) were observed on 5 September 2017 (figure 1(c)), which affected about 83% of the total land area in the Northern Plains. About 23% of the domain was influenced by extreme drought (D3), which induced major crop losses and widespread water shortages (Gerken *et al* 2018).



2.2. Data and methods

2.2.1. ET data summary

Satellite-based ET modeling can provide an effective means for regional monitoring of ET water losses to inform operational water management, agricultural water use conditions (Anderson *et al* 2012) and regional drought assessments (Maes and Steppe 2012, Wardlow *et al* 2017). A consistent and continuous 30 m 8 d cropland ET record was recently developed using a satellite-based ET modeling framework that enables the delineation of field scale cropland water use across CONUS croplands, and is functionally consistent with coarser scale ET assessments available from global operational satellites (He *et al* 2019). The CONUS ET record provides the means for evaluating recent drought related impacts on cropland water use that account for the influence varying crop type conditions.

The 30 m and 8 d CONUS cropland ET record from He *et al* (2019) was extracted for the study domain (figure 1(a)). The ET record extends from 2008 to 2017, and was used to define the climatological conditions for evaluating potentially anomalous cropland water use variations during the 2017 drought relative to the long-term record. The cropland ET product used in this study employs a version of the MOD16 algorithm (Mu *et al* 2011) calibrated for C3 and C4 crop types and driven by finer scale regional

inputs, including 30 m 8 d satellite vegetation cover (e.g. enhanced vegetation index), dynamic land cover from the USDA NASS Cropland Data Layer (CDL), and 4 km daily meteorological data from University of Idaho Gridded Surface Meteorological Dataset (Gridmet; Abatzoglou 2013). The ET product has also been found to provide favorable accuracy for the major CONUS crop types (He *et al* 2019). Unlike the global MOD16A2 record, the CONUS cropland ET record used in this study preserves field scale cropland ET heterogeneity, crop type differences and inter-annual variability across different agricultural fields under varying climate conditions. The 8 d ET anomaly is estimated in this study as the difference between ET estimates in 2017 and the mean 8 d ET climatology established from the 2008–2017 record. The cumulative ET anomalies are calculated as the sum of the 8 d ET anomalies for a given period for the entire study domain. The ET anomalies are extracted for each county in the study domain during the 2017 summer months (June–August) and used for analyzing the spatial and seasonal pattern of drought impacts on cropland water use.

2.2.2. Satellite SIF

Solar-induced chlorophyll fluorescence (SIF) is emitted directly by vegetation as a byproduct of photosynthesis, and provides a close observational proxy of

vegetation status and productivity (Meroni *et al* 2009, Sun *et al* 2017). Global satellite observations of SIF from the ESA GOME-2 (Global Ozone Mapping Experiment 2) sensor have been used as a unique benchmark for agricultural productivity and climate impacts on crop yields (Guanter *et al* 2014, Guan *et al* 2016). The GOME-2 SIF record was able to track the spring onset and autumn termination of photosynthesis indicated by upscaled vegetation gross primary productivity estimates over croplands (Joiner *et al* 2014). The GOME-2 SIF record has also shown drought-related productivity declines, providing an important source of information for regional drought impact assessments (Sun *et al* 2015, Yoshida *et al* 2015). Recently, ground-based SIF measurements were found to correspond closely with plant transpiration (Lu *et al* 2018), owing to similar canopy stomatal controls on both photosynthetic CO₂ exchange and transpiration (Miao *et al* 2018, Yang *et al* 2018).

The monthly 0.5° v27 SIF product (Joiner *et al* 2016) from the GOME-2 instrument on the ESA MetOp-A satellite (<https://avdc.gsfc.nasa.gov/>) was extracted for the study domain and 2008–2017 record. The GOME-2 SIF record was used in this study as a regional indicator of changes in vegetation productivity, but is too coarse to distinguish cropland from other surrounding vegetation communities. The SIF anomalies in 2017 were calculated as differences from a monthly SIF climatology derived from the longer GOME-2 operational record from 2008 to 2017 for each GOME-2 grid cell in the domain. County-level extractions of the GOME-2 SIF anomalies were also compared with similar aggregated cropland ET and NASS county crop production data over the domain.

2.2.3. Other supporting geospatial data

The USDA NASS annual 30 m CDL product was used to characterize spatial and annual variations in crop type and planted area across the study region over the 2008–2017 record (figure 1(b)). Annual county-level crop production data was also obtained from the NASS record to investigate the drought impact on annual cropland productivity across the region in 2017.

The Gridmet meteorological database (Abatzoglou 2013) is derived from temporally rich data from the North American Land Data Assimilation System Phase 2 (NLDAS-2; Mitchell *et al* 2004), and spatially rich data from the Parameter-elevation Regressions on Independent Slopes Model (PRISM; Daly *et al* 2008). Gridmet was used in this study to analyze variations in key regional climate variables over the 2008–2017 record. For analyzing regional climate patterns, the Gridmet daily precipitation was aggregated to coarser 8 d, monthly and annual time steps, while air temperature (Ta) and atmospheric vapor pressure deficit (VPD) were averaged over the same time steps for each grid cell, and then summed or averaged for the entire study region. Precipitation, Ta and VPD anomalies in 2017 were calculated on a grid cell basis as the difference from the

climatological mean values established from the long-term (2008–2017) record. The anomalies were then summed or averaged over the entire Northern Plains domain. Reference ET (ET_{ref}) conditions for alfalfa were obtained using Gridmet daily meteorological inputs, following the methods of (He *et al* 2019). The regional cumulative ET_{ref} was then used with cumulative precipitation to calculate the climate aridity index (AI = precipitation/ET_{ref}), as an indicator of the degree of climate dryness over the study region in 2017. The resulting AI values were grouped into five general climate categories, including hyper-arid (AI < 0.05), arid (0.05 ≤ AI < 0.20), semi-arid (0.20 ≤ AI < 0.5), sub-humid (0.50 ≤ AI ≤ 0.65), and humid (AI > 0.65) conditions (UNESCO 1979).

The regional ET and productivity anomalies in this study were determined using normalized Z-scores to clarify the significance of the 2017 anomalies relative to 'normal' conditions represented by the recent historical record (2008–2017), and for more consistent comparisons among variables with different magnitudes and units. Here, the Z-score is calculated as $Z = (x - \mu)/\sigma$, where x represents the different cropland variables examined, including ET, crop production, and SIF, while μ and σ represent the associated means and standard deviations of these variables, respectively. In contrast, precipitation, Ta and VPD data were not normalized using the Z-score in this study; instead, the cumulative precipitation anomaly was computed as the difference from the long-term (2008–2017) mean, while the number of days and area in 2017 with above-normal Ta and VPD conditions was derived from the long-term record. Pearson's correlation coefficient (r) and the coefficient of determination (R^2) are used in this study as measures of agreement using a 95% significance threshold ($p \leq 0.05$).

3. Results

3.1. Climate conditions in 2017 across the northern plains

The estimated AI from April to September in 2017 indicates that the study region is predominantly semi-arid (AI = 0.24), with a significant drying trend over the 2017 growing season ($r = -0.84$; $p < 0.05$). The greatest dryness (AI = 0.20) is observed in early September, which is also depicted in the USDM (figure 1(c)).

Precipitation was very low for the region in 2017, indicated by large negative anomalies relative to the 2008–2017 record (figure 1(d)). Summer precipitation in the region for 2017 was about 26% below normal conditions and only accounted for 25% of the total annual precipitation. The rapid increase in the number of higher-than-normal Ta and VPD days also indicate generally warmer and drier conditions in 2017 compared to the recent historical record (figure 1(d)). The above results indicate a severe flash drought across the region in 2017, while this study provides an

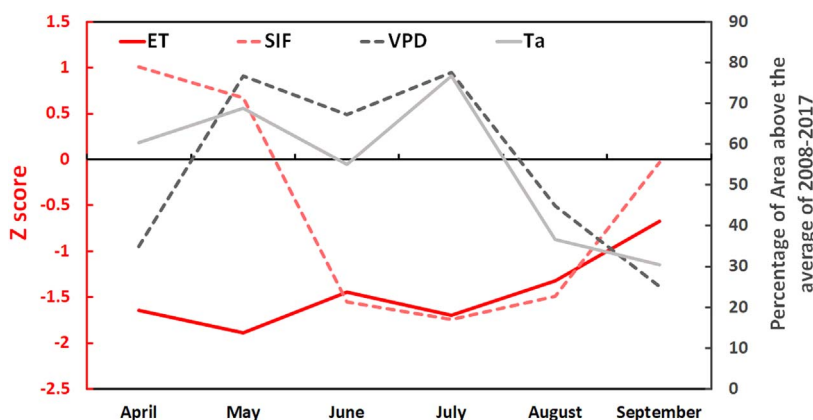


Figure 2. Temporal variations of z-scores of the 2017 growing season cropland evapotranspiration (ET), and solar-induce fluorescence (SIF); and the temporal variations of percentage of area that vapor pressure deficit (VPD) and air temperature (Ta) in 2017 above the average conditions of 2008–2017 in the Northern Plains.

assessment of the associated impact of the drought on cropland ET and productivity.

3.2. Seasonal variation of drought impacts

The satellite-based 30 m 8 d cropland ET estimates in the growing season (April–September) of 2017 all show negative Z-scores, indicating that cropland water use was below-normal relative to the multiyear (2008–2017) average (figure 2). The VPD and Ta records show predominantly positive anomalies encompassing over 25% of the total land area in the domain (figure 2), indicating drier conditions in 2017 relative to the historical period; both parameters accounted for approximately 86% (R^2) of the estimated ET seasonal anomaly in the region. A positive SIF Z-score in April reflects a relatively early growing season onset and enhanced spring productivity in 2017 (figure 2). However, the early growing season onset was followed by a large SIF decline and negative Z-scores from June to August, indicating 16%–18% below-normal summer productivity. Below-normal SIF summer productivity was followed by a return to near-neutral conditions in September coincident with the end of the effective growing season (figure 2). The growing season SIF anomaly is inversely proportional to VPD over the region ($r = -0.58$; $p < 0.05$), indicating reduced productivity under larger atmospheric moisture deficits. However, no obvious relationships were found between SIF and air temperature for the same period.

Cumulative cropland ET anomalies extending from April to September were estimated over the entire Northern Plains in 2017 (figure 3(a)). The resulting ET anomalies show a strong declining regional trend indicating cumulatively lower cropland water use over the 2017 growing season, especially during the summer months. The cumulative ET anomaly was directly proportional to the cumulative precipitation anomaly ($r = 0.90$; $p < 0.05$; figure 3(b)). The negative ET anomalies are exacerbated under drier conditions and reduced in more

humid environments (figure 3(b)), showing significant positive correlations with AI ($r = 0.89$; $p < 0.05$). The SIF anomalies are also directly proportional to cumulative precipitation ($r = 0.67$; $p < 0.05$), cumulative ET ($r = 0.40$; $p < 0.05$), and AI ($r = 0.60$; $p < 0.05$), indicating a strong moisture constraint on vegetation productivity in the region (figure 3(b)).

3.3. Spatial distribution of drought impacts on cropland

About 64% of the Northern Plains region experienced moderate drought (figure 1(c)) by early September of 2017, which coincided with cropland summer ET and SIF observations that were 21% and 19% below normal conditions indicated from the multi-year (2008–2017) record. The associated county-level summer ET, NASS annual crop production and summer SIF Z-scores (figure 4) show general consistency over the Northern Plains counties, with the largest drought related declines in ET (93%), crop production (99%) and SIF (59%) occurring in counties with extensive ranching and dryland agriculture. The NASS reported annual crop production levels for 2017 show large spatial variability across the Northern Plains relative to average conditions indicated from the long-term (2008–2017) record (figures 4(a) and (d)). Most counties (63%) show declines in annual crop production in 2017, with the most severe production decreases (11%–99%) in the north-central and southern portions of the region, where the USDM indicates severe to exceptional drought (figure 1(c)). The cropland ET (figure 4(b)) and SIF records show similar summer reductions (7%–93% and 3%–59%, respectively) in 2017 over the most drought-impacted north-central and southern counties (figure 4(c)). Annual crop production in 2017 shows slight increases in the northeastern counties of the domain (figure 4(a)), where the USDM documents abnormally dry conditions (figure 1(c)). Neutral conditions or small reductions in cropland ET during the summer of 2017 also

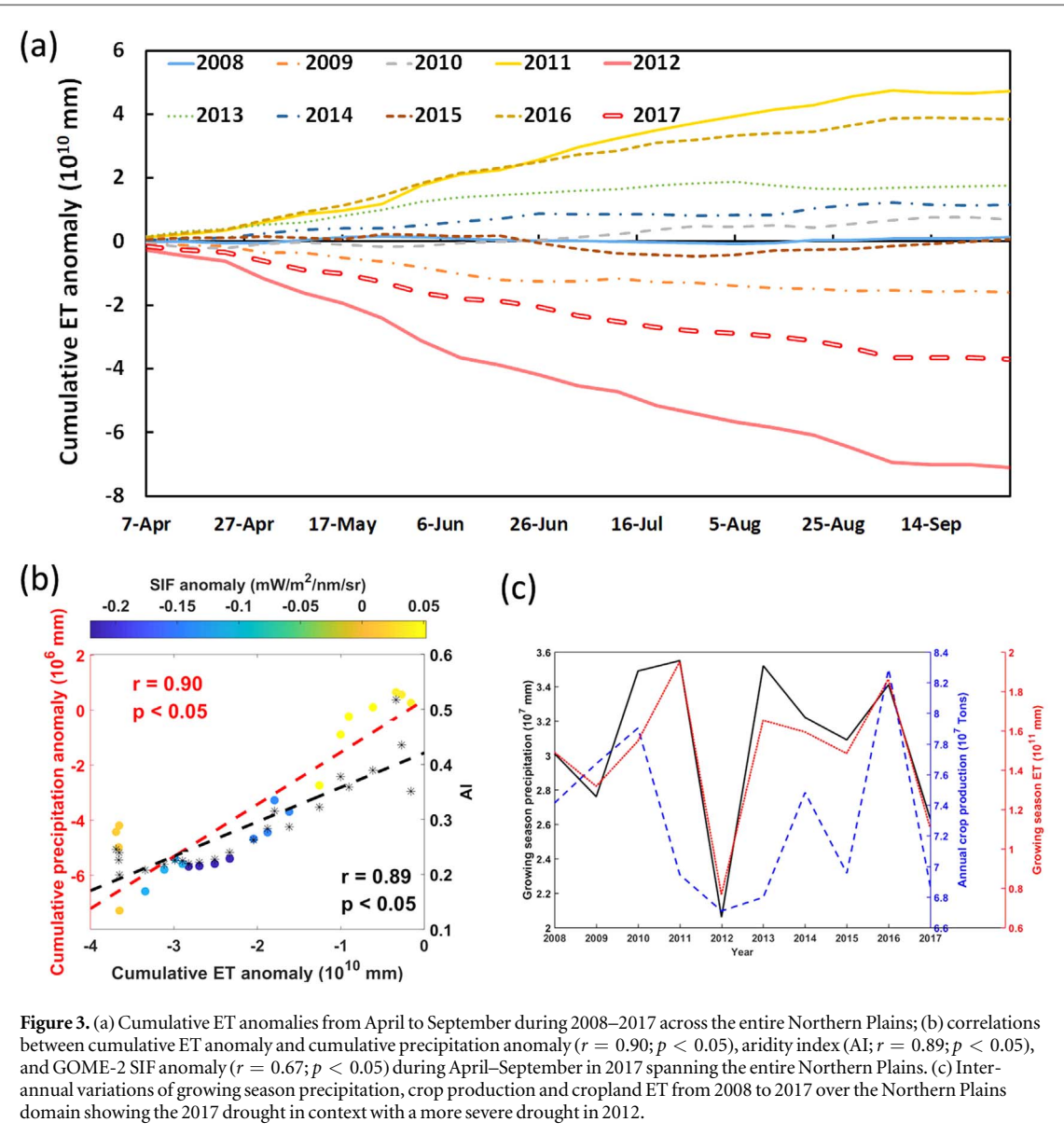


Figure 3. (a) Cumulative ET anomalies from April to September during 2008–2017 across the entire Northern Plains; (b) correlations between cumulative ET anomaly and cumulative precipitation anomaly ($r = 0.90; p < 0.05$), aridity index (AI; $r = 0.89; p < 0.05$), and GOME-2 SIF anomaly ($r = 0.67; p < 0.05$) during April–September in 2017 spanning the entire Northern Plains. (c) Inter-annual variations of growing season precipitation, crop production and cropland ET from 2008 to 2017 over the Northern Plains domain showing the 2017 drought in context with a more severe drought in 2012.

occurred in this region (figure 4(b)). However, the 2017 summer SIF observations over the same region show spatial fluctuations both above and below normal conditions (figure 4(c)). The reported NASS crop production in 2017 (figure 4(a)) also indicates small productivity increases in the southeastern counties of the Northern Plains, where the USDM suggests no apparent drought impacts (figure 1(c)). The 2017 cropland summer ET results show both small positive and negative anomalies in this region (figure 4(b)). However, the 2017 SIF record shows generally less-than-normal summer productivity over the same counties (figure 4(c)). For all Northern Plains counties, the 2017 NASS reported annual crop production Z-scores were positively correlated with estimated cropland summer ET ($r = 0.36; p < 0.05$) and summer SIF ($r = 0.36; p < 0.05$). The above results indicate strong potential for the satellite-driven 30 m

cropland ET estimates to represent cropland drought impacts. The GOME-2 SIF observations also show regional drought-induced productivity declines coincident with lower reported cropland production and ET.

4. Discussion

The 2017 drought (USDM D2-D4) over the Northern Plains affected 46% (7.51×10^7 hectares) of the domain, while counties with extensive ranching and rainfed crops that experienced the most severe summer drought conditions showed 3%–93% and 11%–99% reductions in ET and productivity, respectively. Above-normal precipitation and higher temperature (figure 1(d)) from January to April in 2017 triggered an early spring growing season onset. However, subsequent warmer and drier climate conditions (figures 1(d) and 2) damaged crop

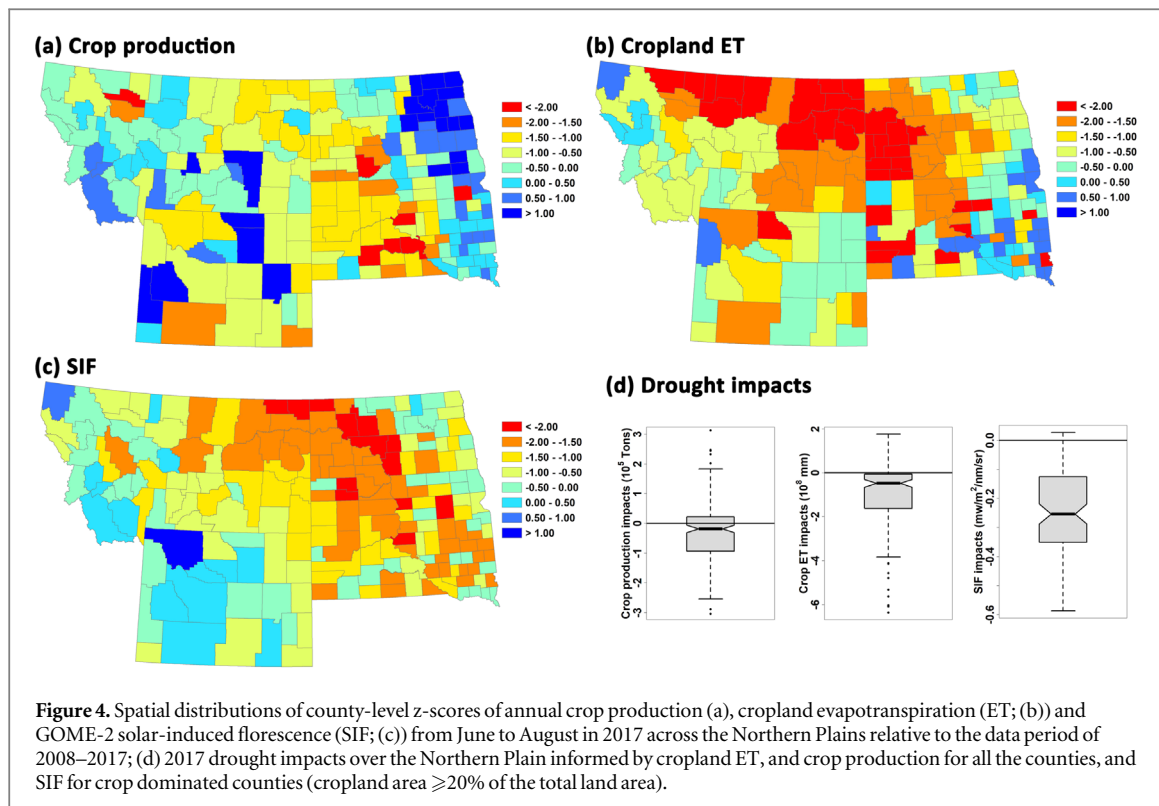


Figure 4. Spatial distributions of county-level z-scores of annual crop production (a), cropland evapotranspiration (ET; (b)) and GOME-2 solar-induced fluorescence (SIF; (c)) from June to August in 2017 across the Northern Plains relative to the data period of 2008–2017; (d) 2017 drought impacts over the Northern Plain informed by cropland ET, and crop production for all the counties, and SIF for crop dominated counties (cropland area $\geq 20\%$ of the total land area).

growth and reduced crop production and ET due to rapidly drying soils over the region. According to the Unified North American Soil Map (Liu *et al* 2013, 2014), the Northern Plains is characterized by predominantly loam soils; whereby, crops grown on these soils may be more susceptible to flash drought due to a rapid reduction in water potential at lower soil moisture levels, reducing crop production and ET. The relatively severe regional reductions in ET and productivity in 2017 indicated from our study coincided with large negative impacts to regional croplands and the agricultural industry, including a 13% decrease in crop values in 2017 relative to average annual crop values from 2008 to 2017, while influencing subsequent management actions to maintain production (Wurster 2018, Wurster *et al* 2019). The drought impact on croplands was likely exacerbated by the extensive rainfed or only partially irrigated agriculture in the region, which is more susceptible to climate extremes.

The different climate factors examined in this study express different impacts on NASS crop production, summer cropland ET and summer SIF regionally. Annual crop production in 2017 was negatively impacted by summer VPD ($r = -0.26$; $p < 0.05$) and Ta ($r = -0.16$; $p < 0.05$) for the Northern Plains. The estimated summer decline in cropland ET in the region also corresponded with larger VPD ($r = -0.58$; $p < 0.05$) and warmer air temperatures ($r = -0.32$; $p < 0.05$), respectively. Summer precipitation across the Northern Plains significantly influenced annual county-level crop production ($r = 0.18$; $p < 0.05$) and summer cropland ET ($r = 0.46$; $p < 0.05$) in 2017. There was no obvious

relationship between summer precipitation and productivity indicated from the SIF record. The limited correlations between the climate factors and GOME-2 SIF record may reflect the scale discrepancy between the coarse (0.5°) footprint SIF observations and finer spatial heterogeneity represented by the 4 km Gridmet climate and 30 m ET records.

The 2017 summer flash drought had a major impact on NP croplands but was less severe than the 2012 Great Plains drought (Hoerling *et al* 2013, Wolf *et al* 2016), which coincided with the driest year of the recent historical record (2008–2017) for the region; whereas, the 2017 event was the second most severe drought for the period of record (figure 3). Growing season precipitation was extremely low in 2012 (figure 3(c)), with more extreme aridity (growing season AI of 0.16 in 2012 versus 0.24 in 2017), and higher growing season VPD and Ta levels than in 2017 or the long-term record (2008–2017). Cropland ET also showed a much lower cumulative anomaly in 2012 (figure 3(a)), while the NASS reported annual crop production was also the lowest in 2012 relative to the other years of record in the region, followed by 2017 (figure 3(c)). The lower crop production in 2012 may also reflect annual variations in crop types and planted area in addition to drought-induced declines. However, the combined results indicated that Northern Plains croplands experienced a more severe drought in 2012 than 2017, which may obscure the impact of the 2017 event due to the more extreme 2012 outlier.

The 30 m cropland ET estimates used in this study are driven by a satellite-based ET model (MOD16

ET algorithm), which has shown favorable regional accuracy in representing field scale cropland ET heterogeneity (He *et al* 2019). However, there are still uncertainties in the ET estimates contributed from input meteorological and land cover data, and algorithm assumptions, which may influence this study. For example, there is no direct soil moisture constraint in the ET algorithm even though ET is strongly sensitive to soil moisture variability (De Lannoy *et al* 2006, Sun *et al* 2013). This lack of a specific soil moisture constraint may contribute to greater model uncertainty at finer spatiotemporal scales where soil and atmospheric moisture conditions may be less correlated (Novick *et al* 2016).

The GOME-2 SIF record shows unique sensitivity to agricultural productivity and climate variability (Guanter *et al* 2014), and demonstrates effective capability for representing drought-related impacts (Yoshida *et al* 2015) despite the coarse scale of the observations. The GOME-2 satellite record also provides global coverage and consistent monitoring capabilities that are particularly useful for areas with sparse ground observations, including the Northern Plains. In this investigation, the SIF observations showed a similar regional drought-induced productivity decline in 2017 consistent with finer scale observations from a satellite 30 m cropland ET record and county-level crop production surveys across the Northern Plains. These records also showed similar climate sensitivity indicated from comparisons with VPD, cumulative precipitation, and AI (figures 2 and 3(b)), confirming that the GOME-2 SIF record is sensitive to drought related impacts on cropland water use and productivity (Liu *et al* 2018, Zhang *et al* 2019). The GOME-2 record has been corrected for sensor degradation (Joiner *et al* 2016), however, remaining artifacts include decreasing inter-annual trends (Zhang *et al* 2018), which may contribute uncertainty to the SIF results from this investigation. While the GOME-2 SIF based assessment of the 2017 drought impact on regional productivity was generally consistent with the finer scale cropland ET and NASS annual crop production assessments the SIF record was unable to distinguish cropland heterogeneity or croplands from other land cover types within a 0.5° resolution grid cell.

Our approach emphasizes global satellite observations to facilitate extrapolations and applications to other regions. Satellite SIF observations have been shown to be sensitive to crop productivity (Guanter *et al* 2014), and used for drought monitoring (Sun *et al* 2015, Yoshida *et al* 2015, Zhang *et al* 2019), though the coarse resolution of GOME-2 SIF records may be a major constraint for effective monitoring over heterogeneous landscapes. Next generation SIF satellites (e.g. TROPOMI; Köhler *et al* 2018) with much finer resolution (e.g. 7 km by 3.5 km pixel with daily visit) may have much greater potential for monitoring ecosystem

productivity response to drought in these heterogeneous regions. The cropland ET and crop production datasets used in this study are largely constrained to the continental US domain due to their reliance on USDA NASS CDL and Gridmet meteorological inputs. However, other synergistic satellite products are available, including the MODIS MOD16A2 ET (Mu *et al* 2011, 2007) and SMAP L4_C productivity records (Jones *et al* 2017), providing moderate (500–1000 m and daily to 8 d) resolution global observations with generally favorable accuracy over croplands, and less ancillary data requirements for potential monitoring and drought impacts assessment in data sparse regions.

5. Conclusion

This study investigates the impact of the 2017 Northern Plains summer drought on regional cropland productivity and ET water losses. The significance of the 2017 summer drought impact was assessed relative to a multi-year observational record (2008–2017) including satellite-driven 30 m cropland ET estimates, NASS annual county-level crop production surveys and GOME-2 SIF regional productivity observations. The extent and severity of the drought indicated from the satellite and NASS records were also evaluated against the USDM. The results indicate that the satellite-based 30 m cropland ET estimates are capable of tracking the seasonal dynamics in the water deficit and evaluating field level cropland drought impacts (figure 3(a)), accounting for approximately 80% of the seasonal dynamics in cumulative precipitation (figure 3(b)). The cropland ET and coarser satellite SIF records showed similar seasonal Z-scores over the region (figure 2), while the SIF anomalies also corresponded strongly with cumulative precipitation ($r = 0.67$; $p < 0.05$), VPD ($r = -0.58$; $p < 0.05$), and AI ($r = 0.60$; $p < 0.05$) during the 2017 growing season. The spatial patterns of Z-scores for annual crop production, summer cropland ET and summer SIF indicate large drought impacts (figure 4) in the north central and southern portions of the domain in 2017, consistent with the USDM assessment (figure 1(c)). The most severely drought impacted area (USDM D2-D4) involved counties with extensive cropland cover, while regions with sparse cropland and a greater proportion of natural vegetation showed more limited drought impacts. Overall, the 2017 drought reduced cropland ET by 25%, crop production by 6% and SIF by 11% across the study domain.

Drought is projected to be more frequent and intense in the future (IPCC 2014). Regional VPD is increasing (Ficklin and Novick 2017), while growing season precipitation is declining and the intervals between precipitation events are increasing (Holden *et al* 2018). This will have direct and immediate

impacts on croplands that can result in major economic losses (Narasimhan and Srinivasan 2005, Howitt *et al* 2014, Martínez-Fernández *et al* 2016). The spatially and temporally complex and dynamic nature of drought constrains capabilities for effective regional monitoring needed for managing water resources and food security risks. This study documents an effective approach for regional drought monitoring in agricultural regions using multi-scale satellite observations that are able to distinguish both field level ET and regional scale productivity changes.

Acknowledgments

This study was funded by USDA NIFA-AFRI and NASA programs (658 2016-67026-25067, NNX14AI50G, NNX14A169G, 80NSSC18K0738). This work used crop production and annual crop value data acquired and shared by the US Department of Agriculture (USDA) National Agricultural Statistics Service (NASS). A portion of this research was carried out at the Jet Propulsion Laboratory, California Institute of Technology, under contract with NASA.

ORCID iDs

Kaiyu Guan  <https://orcid.org/0000-0002-3499-6382>

References

Abatzoglou JT 2013 Development of gridded surface meteorological data for ecological applications and modelling *Int. J. Climatol.* **33** 121–31

AghaKouchak A, Cheng L, Mazdiyasi O and Farahmand A 2014 Global warming and changes in risk of concurrent climate extremes: insights from the 2014 California drought *Geophys. Res. Lett.* **41** 8847–52

Anderson M C, Allen R G, Morse A and Kustas W P 2012 Use of landsat thermal imagery in monitoring evapotranspiration and managing water resources *Remote Sens. Environ.* **122** 50–65

Daly C, Halbleib M, Smith J I, Gibson W P, Doggett M K, Taylor G H, Curtis J and Pasteris P P 2008 Physiographically sensitive mapping of climatological temperature and precipitation across the conterminous United States *Int. J. Climatol.* **28** 2031–64

De Lannoy G J M, Verhoest N E C, Houser P R, Gish T J and Van Meirvenne M 2006 Spatial and temporal characteristics of soil moisture in an intensively monitored agricultural field (OPE3) *J. Hydrol.* **331** 719–30

Ficklin D L and Novick K A 2017 Historic and projected changes in vapor pressure deficit suggest a continental-scale drying of the United States atmosphere *J. Geophys. Res. Atmos.* **122** 2061–79

Ford T W, McRoberts D B, Quiring S M and Hall R E 2015 On the utility of *in situ* soil moisture observations for flash drought early warning in Oklahoma, USA *Geophys. Res. Lett.* **42** 9790–8

Gerken T, Bromley G T, Ruddell B L, Williams S and Stoy P C 2018 Convective suppression before and during the United States Northern great plains flash drought of 2017 *Hydrol. Earth Syst. Sci.* **22** 4155–63

Guan K, Berry J A, Zhang Y, Joiner J, Guanter L, Badgley G and Lobell D B 2016 Improving the monitoring of crop productivity using spaceborne solar-induced fluorescence *Glob. Change Biol.* **22** 716–26

Guanter L *et al* 2014 Global and time-resolved monitoring of crop photosynthesis with chlorophyll fluorescence *Proc. Natl Acad. Sci.* **111** E1327–33

Hao Z, AghaKouchak A and Phillips T J 2013 Changes in concurrent monthly precipitation and temperature extremes *Environ. Res. Lett.* **8** 034014

He M, Kimball J S, Yi Y, Running S, Guan K, Moreno A, Wu X and Maneta M 2019 Satellite data-driven modeling of field scale evapotranspiration in croplands using the MOD16 algorithm framework *Remote Sens. Environ.* **230** 111201

Hoerling M, Eischeid J, Kumar A, Leung R, Mariotti A, Mo K, Schubert S and Seager R 2013 Causes and predictability of the 2012 great plains drought *Bull. Am. Meteorol. Soc.* **95** 269–82

Holden Z A, Swanson A, Luce C H, Jolly W M, Maneta M, Oyler J W, Warren D A, Parsons R and Affleck D 2018 Decreasing fire season precipitation increased recent western US forest wildfire activity *Proc. Natl Acad. Sci.* **115** E8349–57

Horel J D and Dong X 2010 An evaluation of the distribution of remote automated weather stations (RAWS) *J. Appl. Meteorol. Climatol.* **49** 1563–78

Howitt R E, Medellín-Azuara J, MacEwan D, Lund J R and Sumner D A 2014 Economic Analysis of the 2014 Drought for California Agriculture Center for Watershed Sciences (Davis, CA: University of California, Davis, California) (<https://watershed.ucdavis.edu/2014-drought-report>)

Intergovernmental Panel on Climate Change (IPCC) 2014 *Climate Change 2014: Synthesis Report. Contribution of Working Groups I, II and III to the Fifth Assessment Report of the Intergovernmental Panel on Climate Change* ed Core Writing Team, R K Pachauri and L A Meyer (Geneva) (http://ar5-syr.ipcc.ch/ipcc/ipcc/resources/pdf/IPCC_SynthesisReport.pdf)

Joiner J, Yoshida Y, Guanter L and Middleton E M 2016 New methods for the retrieval of chlorophyll red fluorescence from hyperspectral satellite instruments: simulations and application to GOME-2 and SCIAMACHY *Atmos. Meas. Tech.* **9** 3939–67

Joiner J *et al* 2014 The seasonal cycle of satellite chlorophyll fluorescence observations and its relationship to vegetation phenology and ecosystem atmosphere carbon exchange *Remote Sens. Environ.* **152** 375–91

Jones L A *et al* 2017 The SMAP level 4 carbon product for monitoring ecosystem land–atmosphere CO_2 exchange *IEEE Trans. Geosci. Remote Sens.* **55** 6517–32

Köhler P, Frankenberg C, Magney T S, Guanter L, Joiner J and Landgraf J 2018 Global retrievals of solar-induced chlorophyll fluorescence with TROPOMI: first results and intersensor comparison to OCO-2 *Geophys. Res. Lett.* **45** 456–63

Kuwayama Y, Thompson A, Bernknopf R, Zaitchik B and Vail P 2018 Estimating the impact of drought on agriculture using the U.S. drought monitor *Am. J. Agric. Econ.* **101** 193–210

Liu L, Yang X, Zhou H, Liu S, Zhou L, Li X, Yang J, Han X and Wu J 2018 Evaluating the utility of solar-induced chlorophyll fluorescence for drought monitoring by comparison with NDVI derived from wheat canopy *Sci. Total Environ.* **625** 1208–17

Liu S, Wei Y, Post W M, Cook R B, Schaefer K and Thornton M M 2013 The Unified North American soil map and its implication on the soil organic carbon stock in North America *Biogeosciences* **10** 2915–30

Liu S, Wei Y, Post W M, Cook R B, Schaefer K and Thornton M M 2014 NACP MsTMIP: Unified North American Soil Map (Oak Ridge, TN: ORNL DAAC) (<https://doi.org/10.3334/ORNLDAAC/1242>)

Lobell D B, Schlenker W and Costa-Roberts J 2011 Climate trends and global crop production since 1980 *Science* **333** 616–20

Lu X, Liu Z, An S, Miralles D G, Maes W, Liu Y and Tang J 2018 Potential of solar-induced chlorophyll fluorescence to estimate transpiration in a temperate forest *Agric. Forest Meteorol.* **252** 75–87

Luo L and Wood E F 2007 Monitoring and predicting the 2007 U.S. drought *Geophys. Res. Lett.* **34** L22702

Madadgar S, AghaKouchak A, Farahmand A and Davis S J 2017 Probabilistic estimates of drought impacts on agricultural production *Geophys. Res. Lett.* **44** 7799–807

Maes W H and Steppe K 2012 Estimating evapotranspiration and drought stress with ground-based thermal remote sensing in agriculture: a review *J. Exp. Bot.* **63** 4671–712

Martínez-Fernández J, González-Zamora A, Sánchez N, Gumuzzio A and Herrero-Jiménez C M 2016 Satellite soil moisture for agricultural drought monitoring: assessment of the SMOS derived soil water deficit index *Remote Sens. Environ.* **177** 277–86

Meroni M, Rossini M, Guanter L, Alonso L, Rascher U, Colombo R and Moreno J 2009 Remote sensing of solar-induced chlorophyll fluorescence: review of methods and applications *Remote Sens. Environ.* **113** 2037–51

Miao G *et al* 2018 Sun-induced chlorophyll fluorescence, photosynthesis, and light use efficiency of a soybean field from seasonally continuous measurements *J. Geophys. Res. Biogeosci.* **123** 610–23

Mishra A K and Singh V P 2010 A review of drought concepts *J. Hydrol.* **391** 202–16

Mitchell K E *et al* 2004 The multi-institution North American land data assimilation system (NLDAS): utilizing multiple GCIP products and partners in a continental distributed hydrological modeling system *J. Geophys. Res. Atmos.* **109** D07S90

Mo K C and Lettenmaier D P 2015 Heat wave flash droughts in decline *Geophys. Res. Lett.* **42** 2823–9

Mu Q, Heinsch F A, Zhao M and Running S W 2007 Development of a global evapotranspiration algorithm based on MODIS and global meteorology data *Remote Sens. Environ.* **111** 519–36

Mu Q, Zhao M and Running S W 2011 Improvements to a MODIS global terrestrial evapotranspiration algorithm *Remote Sens. Environ.* **115** 1781–800

Narasimhan B and Srinivasan R 2005 Development and evaluation of soil moisture deficit index (SMDI) and evapotranspiration deficit index (ETDI) for agricultural drought monitoring *Agric. Forest Meteorol.* **133** 69–88

Novick K A *et al* 2016 The increasing importance of atmospheric demand for ecosystem water and carbon fluxes *Nat. Clim. Change* **6** 1023

Otkin J A, Svoboda M, Hunt E D, Ford T W, Anderson M C, Hain C and Basara J B 2018 Flash droughts: a review and assessment of the challenges imposed by rapid-onset droughts in the United States *Bull. Am. Meteorol. Soc.* **99** 911–9

Peng B, Guan K, Chen M, Lawrence D M, Pokhrel Y, Suyker A, Arkebauer T and Lu Y 2018 Improving maize growth processes in the community land model: implementation and evaluation *Agric. Forest Meteorol.* **250–251** 64–89

Schroeder R, McDonald K C, Azarderakhsh M and Zimmermann R 2016 ASCAT MetOp-A diurnal backscatter observations of recent vegetation drought patterns over the contiguous U.S.: an assessment of spatial extent and relationship with precipitation and crop yield *Remote Sens. Environ.* **177** 153–9

Sun L, Liang S, Yuan W and Chen Z 2013 Improving a Penman–Monteith evapotranspiration model by incorporating soil moisture control on soil evaporation in semiarid areas *Int. J. Digit. Earth* **6** 134–56

Sun Y, Fu R, Dickinson R, Joiner J, Frankenberg C, Gu L, Xia Y and Fernando N 2015 Drought onset mechanisms revealed by satellite solar-induced chlorophyll fluorescence: insights from two contrasting extreme events *J. Geophys. Res. Biogeosci.* **120** 2427–40

Sun Y *et al* 2017 OCO-2 advances photosynthesis observation from space via solar-induced chlorophyll fluorescence *Science* **358** eaam5747

Svoboda M *et al* 2002 The drought monitor *Bull. Am. Meteorol. Soc.* **83** 1181–90

Trnka M *et al* 2012 Could the changes in regional crop yields be a pointer of climatic change? *Agric. Forest Meteorol.* **166–167** 62–71

Trugman A T, Medvige D, Mankin J S and Anderegg W R L 2018 Soil moisture stress as a major driver of carbon cycle uncertainty *Geophys. Res. Lett.* **45** 6495–503

UNESCO United Nations Educational, Scientific and Cultural Organization (UNESCO) 1979 *Map of the World Distribution of Arid Regions: Map at Scale 1:25000000 with Explanatory Note*. (MAB Technical Notes 7 (Paris: UNESCO)

Wang Q *et al* 2014 Temporal-spatial characteristics of severe drought events and their impact on agriculture on a global scale *Quat. Int.* **349** 10–21

Wardlow B D, Anderson M, Hain C, Crow W, Otkin J, Tadesse T and AghaKouchak A 2017 Advancements in satellite remote sensing for drought monitoring: integrating science, management, and policy *Drought Water Crises* (London: Taylor & Francis) ch 10 pp 225–8

Wolf S *et al* 2016 Warm spring reduced carbon cycle impact of the 2012 US summer drought *Proc. Natl Acad. Sci.* **113** 5880–85

Wurster P M 2018 Understanding the Food Water Nexus: characterizing THE IMPACT OF climatological anomalies on agrosystems (Missoula, MT: University of Montana)

Wurster P M *et al* 2019 Characterizing the impact of climatic anomalies on agrosystems in the northwest United States *Agric. Forest Meteorol.* (submitted)

Yang X, Shi H, Stovall A, Guan K, Miao G, Zhang Y, Zhang Y, Xiao X, Ryu Y and Lee J-E 2018 FluoSpec 2—an automated field spectroscopy system to monitor canopy solar-induced fluorescence *Sensors* **18** 2063

Yoshida Y, Joiner J, Tucker C, Berry J, Lee J E, Walker G, Reichle R, Koster R, Lyapustin A and Wang Y 2015 The 2010 Russian drought impact on satellite measurements of solar-induced chlorophyll fluorescence: insights from modeling and comparisons with parameters derived from satellite reflectances *Remote Sens. Environ.* **166** 163–77

Zhang L, Qiao N, Huang C and Wang S 2019 Monitoring drought effects on vegetation productivity using satellite solar-induced chlorophyll fluorescence *Remote Sens.* **11** 378

Zhang Y, Joiner J, Gentile P and Zhou S 2018 Reduced solar-induced chlorophyll fluorescence from GOME-2 during Amazon drought caused by dataset artifacts *Glob. Change Biol.* **24** 2229–30

Zhao M and Running S W 2010 Drought-induced reduction in global terrestrial net primary production from 2000 through 2009 *Science* **329** 940–3